Parallel dynamics of slow slips and fluid-induced seismic swarms

Philippe Danré, Louis de Barros, Frédéric Cappa, Luigi Passarelli

nature communications

Article

https://doi.org/10.1038/s41467-024-53285-3

Parallel dynamics of slow slips and fluid-induced seismic swarms

Received: 12 March 2024

Accepted: 8 October 2024

Published online: 17 October 2024

Check for updates

Philippe Danré[1] ✉, Louis De Barros[1], Frédéric Cappa[1] & Luigi Passarelli[2]

Earthquake swarms may be driven by fluids, through hydraulic injections or natural fluid circulation, but also by slow and aseismic slip transients. Understanding the driving factors for these prolific sequences and how they can potentially develop into larger ruptures remains a challenge. A notable and almost ubiquitous feature of swarms is their hypocenters migration, which occurrence is closely related to the processes driving the observed seismicity, in a similar way as seismicity accompanies slow-slip events at subduction zones. Here, we analyze global data on migrating sequences, and identify scaling laws for migration velocity, moment and duration measured on natural and injection-induced swarms, foreshock sequences, and slow slip events. We highlight two different behaviors among these sequences: one linked to slow slips, with elevated migration velocities and moments, and the other related to fluid-induced processes, featuring lower velocities and moments. These results provide metrics for distinguishing between the drivers of earthquake swarms, fluid or slow-slip related, and prompt a reevaluation of scaling laws of fault slip transients, especially for swarms.

Slip along faults can be seismic or aseismic, and occurs at various scales of fault size, slip released or source duration. Ruptures can span hundreds to thousands of kilometers[1,2] and last from seconds to months[2,3]. To gain insights into the processes occurring during slip episodes, scaling laws have been widely used to compare observations at the micrometer scale in laboratory[4] to slip events that extend for hundreds of kilometers[1]. Typical representations of slip duration (T) as a function of released moment (M_O)[5,6] revealed two different scaling laws. Individual earthquakes follow the scaling law $M_0 \propto T^3$ across more than four orders of magnitude[3], whereas slow slip events and transient aseismic slip sequences observed in subduction zones, exhibit a $M_O \propto T$ dependence[5], although recent observations indicate that locally, a $M_0 \propto T^3$ scaling can emerge in SSE sequences[7,8]. Nevertheless, these scaling relations are of significant importance and subject to debate as they provide fundamental information about the physics of fault slip[9,10].

Another crucial parameter of interest lies in the velocity at which transient slip episodes migrate over time. In subduction zones, slow slip events have been observed to propagate at velocities of a few kilometers per day[2], occasionally accompanied by faster transients known as secondary slip fronts[11]. Conversely, some episodes of seismicity migrate only a few meters per day[12]. This phenomenon is also characteristic of earthquake swarms, which are prolonged sequences of seismic activity lacking a distinct mainshock. Swarms manifest in diverse settings, including subduction zones[13], rift areas[14], mountain ranges[15–17], and intraplate regions[18]. They can also be induced by fluid injections during industrial activities such as Enhanced Geothermal System (EGS) development, carbon dioxide or wastewater storage[19–22]. Some earthquake swarms exhibit complex migration patterns, where alongside the overall migration of the sequence, faster and shorter seismicity transients have been observed and interpreted as indicative of aseismic slip[14,23]. Moreover, swarm-like seismicity can escalate into large earthquakes[24] and is retrospectively identified as a foreshock sequence which also exhibits migration patterns that unveil its underlying driving processes[24–26].

Swarms or foreshock sequences can persist for days to years, suggesting the need of an external driving force to sustain the seismicity rate and its migration. Studying seismicity migration

[1]Université Côte d'Azur, CNRS, Observatoire de la Côte d'Azur, IRD, Géoazur, Sophia Antipolis Valbonne, France. [2]INGV - Istituto Nazionale di Geofisica e Vulcanologia, sezione di Bologna Viale Berti Pichat 6/2, Bologna, Italy. ✉e-mail: philippe.danre@geoazur.unice.fr

conventionally involves the use of distance-time plots (Fig. 1) and has led to various mechanisms proposed to explain it, including pore pressure diffusion[27], poro-elastic deformation[28], earthquakes interactions[29] or transient aseismic loading[14,30–32]. Understanding the relation between migration velocity (V) and duration (T) can provide insights into these processes. For instance, migration following a fluid pressure diffusion law may exhibit a scaling of $V \propto T^{-0.5}$, while linear migration may indicate fluid-induced aseismic slip[30,31,33]. The absence of migration would be characterized by $V \propto T^{-1}$.

Recent studies focusing on swarms have revealed that their migration velocities scale across a wide range of magnitudes, notably with swarm duration for both natural and injection-induced sequences lasting from a few days to several years[30,34]. Conversely, certain swarms observed in subduction or transform faults display significantly higher

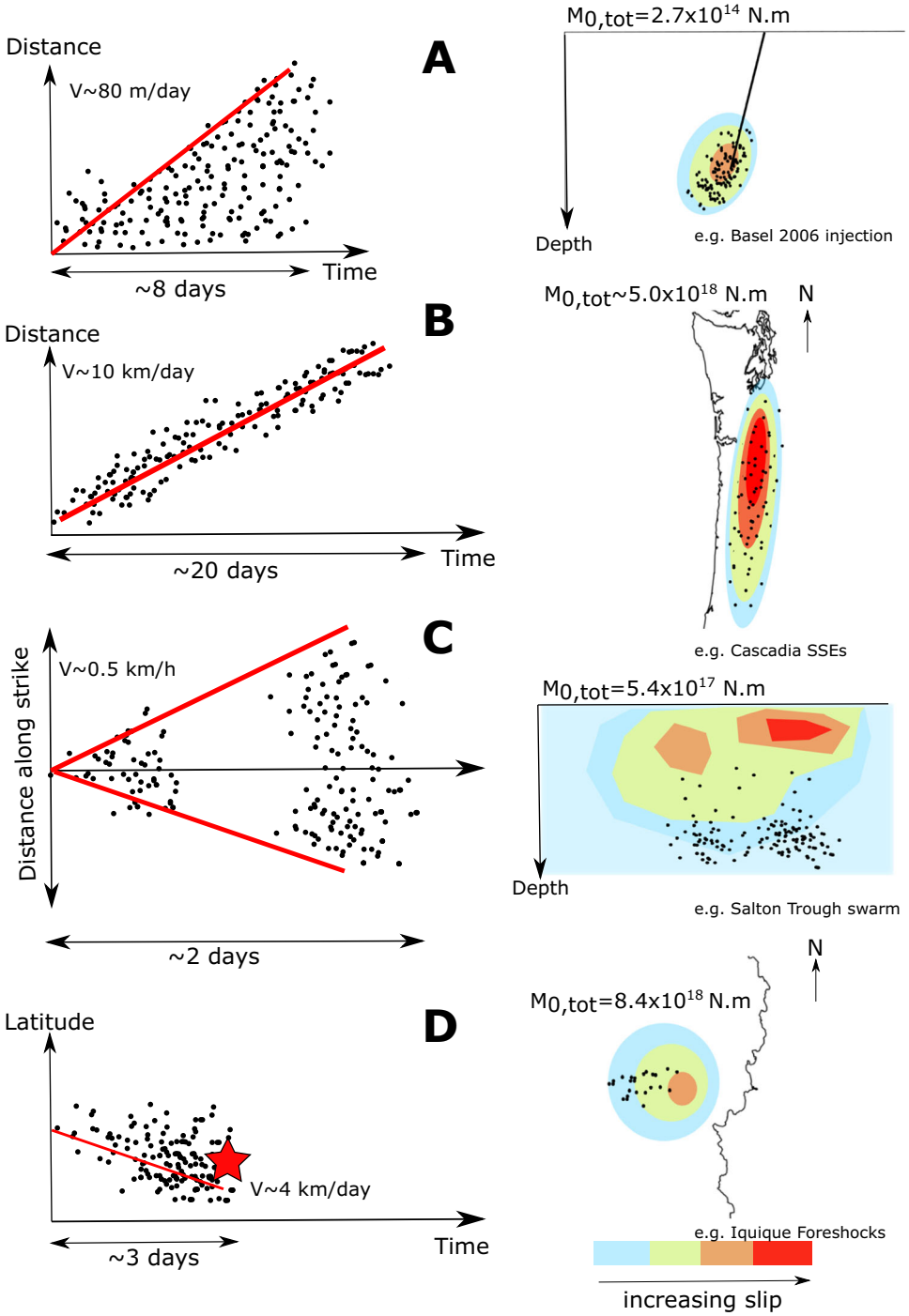

Fig. 1 | Simplified schematic representations of various seismicity migration episodes. The left column of the figure shows the distance or positions of earthquakes (or tremors for Cascadia) over time, represented by black points. The red line illustrates the observed migration pattern with an approximate velocity *V*. The right column displays the schematic slip distribution during these episodes with the associated moment value $M_{0,tot}$. **A** Swarm induced by the development of an Enhanced Geothermal System near Basel, Switzerland, in 2006[63,64]. **B** Slow slip episode (SSE) in the Cascadia subduction area, USA[65,66]. **C** Earthquake swarm occurring on a transform fault in the Salton Trough, USA[32,41]. **D** Foreshocks of the $M_w = 6.9$ Valparaiso earthquake in 2017 in Chile[40]. It is important to note that, for Basel swarm, the slip shape is inferred from a noise-based study of deformation[64] as no direct geodetic measurement have been conducted. Indicative coastlines contours were drawn using Python's matplotlib basemap.

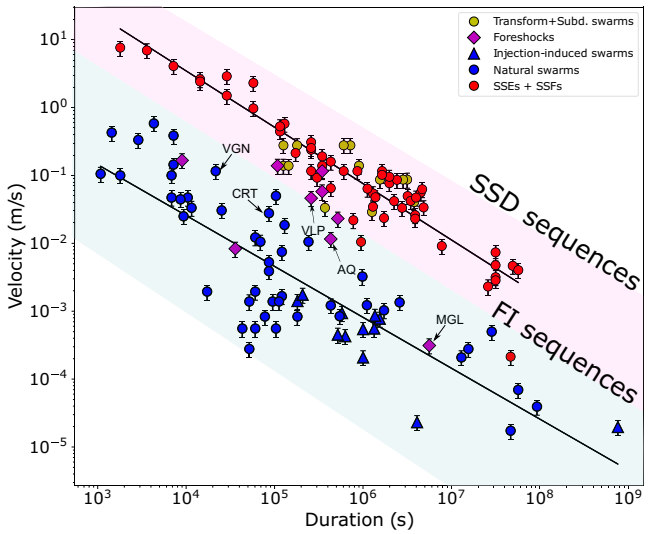

Fig. 2 | Migration velocity as a function of duration for the various types of FI and SSD sequences. Migration velocity is determined based on the migration rate of earthquakes in swarm sequences, or the propagation rate of tremor, low frequency earthquake or slip in slow slip events and secondary slip fronts. In the plot, blue points represent natural swarm sequences, while triangles denote injection-induced sequences. Purple circles represent foreshock sequences, with specific names highlighted for some of them (VLP, AQ, MGL are Valparaiso (2017), l'Aquila (2009) and Mogul (2008) foreshock sequences, respectively). CRT and VGN indicate two fast seismicity bursts occurring during the 2015 Corinth earthquake swarm and the 2014 Virginia City sequence[14,23]. Red points indicate Slow-slip events (SSEs) or Secondary Slip fronts (SSFs), while yellow points represent swarms on subduction or transform faults (see Supplementary Materials for more details). Error bars correspond to an uncertainty of 25% of velocity value for all sequences. The thick black lines represent the best-fit lines obtained for fluid-induced and slow slip driven sequences, showcasing the overall trend observed in the data. The pink and blue areas arbitrarily illustrate the scaling relationships for SSD (slow slip driven) sequences and FI (fluid-induced) swarms, respectively.

migration rates, and behave more like Slow-Slip Events (SSEs)[32,35]. Therefore, fluid-induced swarms and SSEs may represent the two extreme behaviors of migrating seismic sequences[30].

Echoing the substantial body of work existing on the scaling of duration with moment for SSEs and earthquakes, investigating potential scaling of migration velocity with duration is also crucial for understanding slip transients on a global scale[30]. We here employ scaling laws to compare migrating sequences from a global dataset of swarms and foreshocks with slow-slip events, secondary slip front and other fast migrating seismic sequences. By doing so, we aim at identifying their common characteristics, shedding light on their triggering processes, and gaining a better understanding of their driving mechanisms.

Results

A bimodal continuum of migration velocities

A plot of the migration velocities against the durations of earthquake sequences studied here shows two distinct trends despite having similar slopes (Fig. 2). The first trend, characterized by high migration velocities, includes slow slip events (SSEs), secondary slip fronts (SSFs), as well as some swarms from subduction and transform fault zones (Fig. 2). For clarity, we refer to this group as *"slow slip driven"* (SSD) sequences, given that the majority have an underlying slow slip trigger. The second trend corresponds to injection-induced swarms and swarms taking place in diverse contexts like rift zones or mountain ranges (see Table S1), labeled as *"natural"* earthquake swarms here, and certain foreshock sequences. We call this group *"fluid-induced"* (FI) sequences due to the presence of all injection-induced sequences. Note that we do not exclude the role of fluids in the dynamics of SSD sequences. In both cases, we observe a scaling relationship of $V \propto T^{-\alpha}$ over a duration range spanning six orders of magnitude (Fig. 2). For FI swarms, we find $\alpha = 0.75 \pm 0.15$ for a 95% confidence threshold computed assuming a Gaussian distribution of errors, while for SSD sequences, we obtain $\alpha = 0.81 \pm 0.08$ (Fig. 3A).

Despite exhibiting a similar dependence of velocity with duration, the two groups display significantly distinct positions along the ordinate axis (Figs. 2 and 3B). Assuming an exponent $\alpha = 0.8$, the distribution of the parameter $\varphi = \log(V \times T^{\alpha})$ clearly exhibits a bimodal distribution (Fig. 3C), indicating two distinct and well-separated behaviors. On average, FI sequences have an intercept of $\varphi_{mean} = 1.5 \pm 0.6$, indicating velocities two orders of magnitude slower than SSD sequences, which have an average $\varphi_{mean} = 3.7 \pm 0.4$. Therefore, SSD sequences show higher migration velocities compared to FI swarms, by two orders of magnitude. For instance, taking a week-long duration, SSD sequences can reach migration velocities of several tens of kilometers per day, whereas injection-induced swarms typically exhibit velocities in the range of hundreds of meters per day (Fig. 2). If the mechanism controlling seismicity migration is common to SSD and FI, as shown by the slope values, such differences in the scaling intercept might be explained by a systematic difference in the parameters involved in migration dynamics. While prior research has already identified a distinction between swarms and SSEs[30], this study underscores a broader spectrum of behaviors within migrating sequences, leveraging a larger and more diverse dataset.

The apparent scattering of data points in Figs. 2 and 3C may arise from complexities in the migration patterns that are not captured by an average velocity or from a difference in velocity determination methodology. It might also reveal a 2nd order dependency on fault and hydraulic properties, such as fault criticality concerning the stress state[36], or physical factors like frictional properties, temperature and fluid pressure[35].

This parallel, but distinct, behavior provides a valuable observable for distinguishing between the two groups and for inferring their driving processes. Migration velocity alone cannot make this distinction, as previously done[32,37], since short-duration swarms may exhibit faster migration than long-duration SSD sequences (Fig. 2). However, velocity-duration relations can be used to determine the main driving mechanisms of the swarm. For instance, the foreshocks of the 2008 $M_w = 4.9$ Mogul and those of the 2009 $M_w = 6.3$ L'Aquila earthquake sequences[24,38] appear to behave like FI-swarms (Fig. 2), indicating that their dynamics align with injection-induced seismicity episodes. This would also be the case of the seismicity preceding the 2023 and 2024 Noto earthquakes, which migrates of ~8 km in depth for ~650 days before the first $M_w = 6.2$ earthquake[39]. Some fast seismicity transients (VGN and CRT, see Fig. 2) occurring during earthquake swarms, within the global earthquake migration, have been thought to be a direct signature of underlying aseismic slip based on their elevated migration velocity alone[14,23]. However, contrary to previous interpretations based solely on their elevated migration velocity, our results suggest that these fast seismicity transients share the same underlying driving mechanisms as those governing the overall sequence migration, as they scale within FI sequences rather than SSDs (Fig. 2).

Conversely, the migration of the precursory events of the 2017 $M_w = 6.9$ Valparaiso earthquake[40] and the 2014 $M_w = 8.1$ Iquique earthquake[26] confirm that these sequences are driven by slow slip. Figure 2 also further confirms that swarms occurring on transform faults[41,42] are primarily driven by slow slips rather than fluid-induced processes, as their migration behavior falls precisely within the patterns observed for SSEs.

The extensive dataset, encompassing numerous sequences with a wide range of durations and velocities, along with the diversity of

https://doi.org/10.1038/s41467-024-53285-3

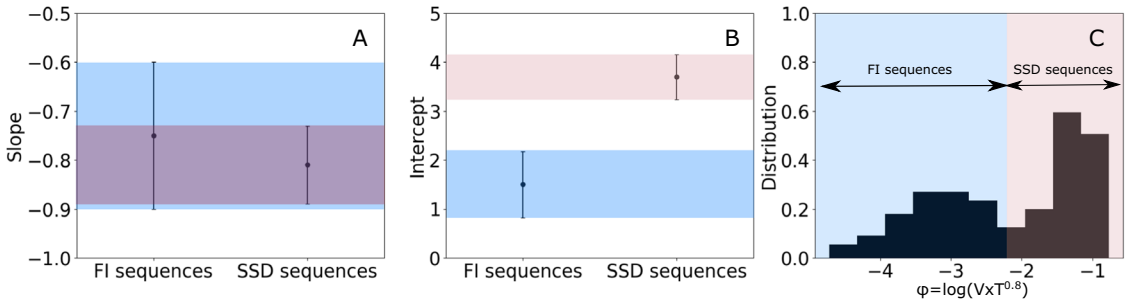

Fig. 3 | Statistical details of the scaling between velocity and duration. A Values of slope obtained for swarms (blue points on Fig. 2) and SSEs+SSFs (slow slip events + secondary slip fronts, red points on Fig. 2). **B** Same but for intercept values. Error bars indicate slope or intercept values intervals for a 95% confidence threshold computed assuming a Gaussian distribution of errors. **C** Distribution of the parameter $\log(V \times T^{\alpha})$ for the sequences examined in Fig. 2. The light blue area indicates FI (fluid-induced) sequences, while the pink area denotes SSD (slow slip driven) sequences. Those areas are drawn for illustration purposes, as an overlap between both types of sequences may exist.

tectonic contexts and types of sequences examined, results in a more robust estimate of α compared to previous studies[30]. The inferred exponents ($\alpha \sim 0.8$) for both FI and SSD sequences notably deviate from $\alpha = 0.5$ which is characteristic of a diffusive pattern. This deviation is corroborated by the apparent diffusivity coefficient, derived from fitting a diffusion law to migration fronts[33,43], which exhibits a dependency on swarm duration[44] (see Figure S1). Such a dependence, in addition to the value of $\alpha \sim 0.8$ determined here make a diffusive relationship between time and distance, leading to a $V \propto T^{-0.5}$, less plausible.

The similarity in α for FI and SSD sequences suggests that a common mechanism may be responsible for the migration of slip, seismicity or tremors in the two groups. Aseismic slip has been directly measured for SSD sequences such as SSEs, as well as in some earthquake swarms[41], foreshocks[45], and injection experiments[46], and is also expected based on numerical modeling[47]. Theoretical findings for specific FI sequences have obtained similar α values to those determined here[31], assuming that aseismic slip drives seismicity migration. Therefore, the common $V \propto T^{-\alpha}$ scaling observed for FI and SSD supports the idea that both types of sequences may be driven by aseismic slip. In FI sequences, this aseismic slip is fluid-induced[46,48], with the migration velocity actually corresponding to the rupture velocity of this aseismic transient.

Moment duration scaling highlights two distinct behaviors

While studying migration velocities provides insights into two distinct regimes, a more conventional approach for discriminating slip sequences involves analyzing moment and duration, as it also provides information about the magnitude of the deformation. However, representations that solely consider seismic moment as a function of duration for swarms are incomplete, as aseismic moment release occurs during swarms[41,49,50] and can sometimes exceed seismic moment by several orders of magnitude[30,35]. This was assessed in previous studies looking at the ($T-M_{O,seismic}$) scaling for swarms[51] where the absence of a clear scaling is explained by not taking into account aseismic moment released. Consequently, in our analysis, we consider the total moment (seismic and aseismic) in the scaling representations and compare it to duration (Fig. 4). When deformation is too subtle to be detected by geodetic measurements, we estimate the total moment by drawing analogies with repeating events and creep episodes[30,52]. Here, we assume that seismic slip serves as a proxy for the surrounding aseismic slip. By using the seismic slip associated with the largest event of a sequence, we can estimate the average slip over the entire swarm area. This approach enables the reconstruction of the total moment released during the studied sequence[30], overcoming the detectability challenges posed by conventional geodetic methods. This method has been validated using values from the literature[30] or through injected fluid volume reconstruction[53].

From Fig. 4, it appears that, as for the migration velocity-duration relation, the FI swarms exhibit an alignment parallel to the SSD sequences, with a $M_O \propto T$ scaling. It confirms that SSD and FI swarms share similarities in their driving processes. The $M_O \propto T$ scaling has been commonly observed on compilations of slow slip events[5,54]. While individual sequences of slow slip events or low frequency earthquakes may exhibit a scaling relationship of ($M_0 \propto T^3$)[7,8,55], the global trend of $M_O \propto T$ arises from the compilation of these individual scalings[5,47]. Therefore, by analogy with SSD, one might actually wonder if $M_0 \propto T^3$ transients might be observed within individual FI sequences despite the observed global scaling.

The two groups are also distinctly separated, as the total moment released during FI swarms is approximately three to four orders of magnitude lower than that of SSD sequences for a given duration. This offset between both group scalings exceeds the estimated moment uncertainty of 1 order of magnitude here (see Supplementary Materials Text S1), and is not related to the size of the swarms or the background stress level. For example, the 2005 Salton Trough[41] and 2013-2014 Apennines[49] swarms share similar size and depth (indicating similar confining stress levels), yet they belong to SSD and FI sequences, respectively. The parallel scaling observed between the FI and SSD sequences in both moment and duration, along with the analogous pattern noted between migration velocity and duration (Fig. 2) may also manifest in the relation between moment and migration velocity. However, this association might entail more underlying uncertainty due to the methods and assumptions employed to compute both parameters (see Fig. S2), resulting in a less distinctly discernible trend.

For most FI swarms, the total moment could only be estimated[30], which limits the depth of analysis. However, in specific cases where the total moment was precisely quantified through geodetic measurements, it confirms the aforementioned observation[35,41,49,56,57]. For example, the 2013–2014 Apennines[49] and 2012 Pollino range[35] swarms, where the total moment was measured through geodesy, align with the FI swarms (Fig. 4). Conversely, certain swarms, such as the 2005 Salton Trough sequence[41] and the Iquique precursor foreshock sequence exhibit behavior similar to SSEs, which reinforces the dichotomy made in Fig. 2 based on their observed migration velocity and duration. In conclusion, Fig. 4 introduces the distinction of two slip modes, corresponding to sequences of migrating slip or seismicity, highlighted by different $M_O \propto T$ scalings: slow-slip driven sequences and fluid-induced swarms. This indicates that previous scaling representations only considering earthquakes and SSEs in the slip spectrum are incomplete by missing all FI sequences[54].

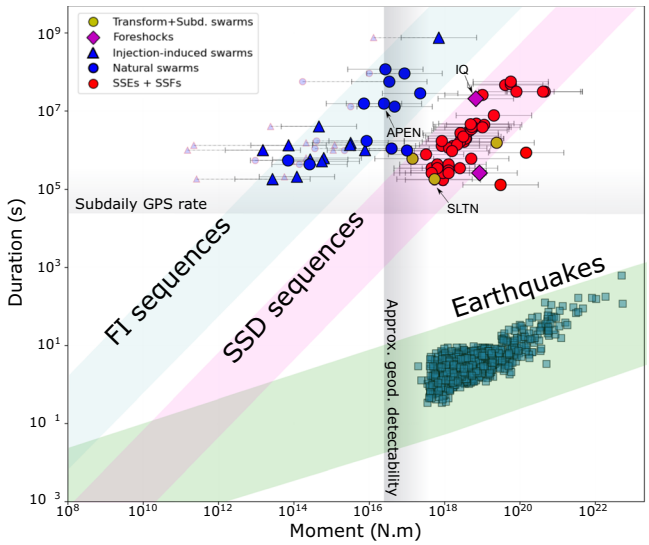

Fig. 4 | Duration – moment scaling for the various types of seismic sequences. Blue triangles correspond to the estimated total moment of injection-induced swarms, as determined by Danré et al. [30]. Blue circles represent natural swarms, with the total moment either estimated or measured using geodetic data (see table S1). The shaded symbols indicate the seismic moment – duration, with a dashed line connecting the seismic and total moments. Red and yellow circles represent the measured total moment for SSEs (slow slip events) and subduction or transform fault swarms (when available), respectively. Error bars are represented assuming a maximum 1 order of magnitude uncertainty in total moment determination for all sequences. Squares represent seismic moment and duration data obtained from a global earthquake dataset. The duration is determined through corner frequency analysis of nearly a thousand of earthquakes[3]. The green, pink and blue areas arbitrarily illustrate the scaling relationships for earthquakes, SSD (slow slip driven) sequences and FI (fluid-induced) swarms, respectively. SLTN Slaton Trough swarm[41], IQ Iquique precursor episode[45], APEN Apennines swarm[35], SSF secondary slip front.

Discussion

By analyzing migration velocity-duration and duration-moment relationships within a global dataset of migrating slip sequences, we identify two distinct behaviors among migrating seismicity episodes: (1) fluid-induced –FI– and (2) slow slip driven –SSD– sequences. This contributes to draw a more complex picture than the usual understanding of transient slip episodes with just slow slip episodes distinct from earthquake ruptures, as FI sequences are a well-defined category of events in the moment-duration domain.

These scaling relations provide straightforward tools to differentiate the driving mechanisms of swarms. Our observations confirm that the preparatory phase of the 2009 $M_w = 6.3$ L'Aquila earthquake[24] was driven by fluid processes similar to what happens during the induced seismicity observed in the 1993 Soultz-sous-Forêts sequence for instance[58]. Also, even if fast migration episodes observed within some FI swarms[14,23] were primarily attributed to fast aseismic transients, they follow the same laws as global FI sequences migrations. Furthermore, FI natural swarms, FI foreshocks sequences, and anthropogenic seismicity exhibit similar scalings (Figs. 2 to 4), suggesting here a common underlying mechanism. Consequently, bridging observations from these different types of sequences holds promise for gaining insights into driving mechanisms and relevant unknowns, such as on fluid circulation dynamics[53,59] and physical fault characteristics like fault toughness or frictional parameters[31].

While it is expected that some subduction swarms share similarities with SSEs due to their similar tectonic context, it is less straightforward to argue the same for swarms on transform faults. They exhibit shallow ruptures on nearly vertical faults, whereas SSEs generally occur at greater depth on the subduction interface. However, scaling relations examined in this study demonstrate that both subduction and transform fault swarms behave similarly to SSEs (Fig. 2). This indicates similarities in their underlying physics, thereby implying the need to bridge the extensive observations and modeling conducted individually on those sequences to fully explain the features observed in all SSD sequences.

A more general mechanism is needed to explain the distinction between FI and SSD sequences. For instance, in FI swarms, aseismic slip is presumably induced by an increase in fluid pressure[46,47,60]. In contrast, for SSD swarms, fluid circulation does not seem to be required. However, increased pressure within the faults may still trigger slow aseismic slip by increasing the earthquake nucleation length[61].

The scaling laws obtained in this study are compatible with previous research focusing on moment and duration[5] with $M_{0,total} \propto T$ or on moment and velocity[35] (Figure S2). Moreover, incorporating fluid-induced sequences (FI) in our study adresses observational gaps identified in the literature[54], thereby defining an ensemble that runs parallel to SSEs. Several first-order hypotheses have been proposed to explain the moment-duration scaling for SSEs, and could therefore explain observations made in Figs. 2 and 4. Among these models, those involving either uniform slip or uniform stress drop are consistent with the $M_0 \propto T$ scaling observed here[5]. These models yield a dependence of length (L) on duration (T) of $L^2 \propto \mathrm{T}$ and $L^3 \propto \mathrm{T}$, respectively, resulting in values of $\alpha = 0.5$ or $\alpha = \frac{2}{3}$, respectively, in the $V \propto T^{-\alpha}$ scaling[5]. However, these exponents appear lower than those observed in our study, even when considering the significant scattering (Fig. 3). In particular, we can reject a diffusive relation ($\alpha = 0.5$), commonly assumed for FI sequences. An alternative explanation for Figs. 2 and 4, by considering $M_0 \propto T$ and $V \propto T^{-0.75}$, suggests $M_0 \propto R^4$, indicating slip that grows with the surface area of the sequence.

Precisely determining the value of α and providing a comprehensive global explanation for the observed scalings presents a challenge due to the dispersion of data points. To address this, standardizing the methodology for determining velocity, duration, and moment could enhance the precision of observations in this study. This standardization would facilitate the development of precise metrics for quantifying uncertainties and potentially reduce the uncertainties observed in velocity and moment scaling with duration.

Achieving this would require implementing state-of-the-art detection location and relocation techniques to ensure accurate measurements of these parameters, by using openly available waveform data. Alternatively, examining the systematic differences between FI and SSD sequences, considering factors such as tectonic context, fluid presence and pressurization (e.g., during fluid injections) might provide valuable insights towards developing a generic model for migrating slip transients.

Methods

We have compiled a comprehensive global dataset that encompasses seismic catalogs of various migrating sequences. This dataset contains twelve sequences induced by injection activities in geothermal systems and wastewater disposal, as well as over fifty natural swarms occurring in diverse tectonically active regions like mountain ranges[16], rift zones[14], subduction zones[13] and transform faults[41]. Additionally, we have included two examples of fast seismicity bursts occurring during swarms[14,23] as well as notable sequences of foreshocks, observed in subduction areas[26,40,45] and transform[25] and normal fault systems[24]. We have also incorporated observations of slow-slip events from subduction zones based on the SSEs catalogs from Gao et al.[2] and secondary slip fronts (SSF) as documented by Bletery et al.[11]. The diversity of tectonic or industrial fluid injection contexts, combined with a wide range of durations (spanning over 6 orders of magnitude, see Fig. 2), velocities (also covering over 6 orders of magnitude, see Fig. 2) and moments (encompassing over 7 orders of magnitude), alongside the various natures of migrating slip sequences (including SSEs, SSFs,

swarms, fast transients, foreshocks), as well as the potential mechanisms proposed to explain such migrations (pressure diffusion[28], aseismic slip[32], poro-elastic effects[28]), collectively contribute to a dataset that offers a more comprehensive representation of migrating slip sequences compared to previous works[30]. From all these studies, we compile values of the migration velocity of seismicity and tremors, the duration of the migrating sequence and, when available, the total moment associated. Error estimates for velocity and moment are often unavailable or challenging to compute from the works considered, as these values are derived using various methods (like for velocity: direct fitting[62], seismicity front fitting[30], direct estimate[32]). To maintain consistency across all datasets used in this study and align with previous research on scaling laws facing similar challenges, we adopt a conservative approach. We assigned a migration velocity uncertainty of 25% and a total moment error of up to 1 order of magnitude[2]. However, it is likely that the error is lower for geodetical moments, especially in more recent studies, due to improvements in GPS coverage and the quality of InSAR data. Errors in duration are neglected as they are likely to be small compared to those of velocity and moment. Indeed, migration duration is almost identical to injection duration for injection-induced sequences[53] while seismicity duration and geodetic duration are also closely correlated[35]. This correlation makes the determination of transient slip episodes duration reliable through the compiled values here. Detailed information on data sources, corresponding values, and uncertainties used in our analysis can be found in Supplementary Tables S1 and S2 and Text S1.

Data availability

All data and corresponding sources are available in the Supplementary Materials, Table 1.

References

1. Ammon, C. J. et al. Rupture process of the 2004 Sumatra-Andaman Earthquake. *Science* **308**, 1133–1139 (2005).
2. Gao, H., Schmidt, D. A. & Weldon, R. J. Scaling relationships of source parameters for slow slip events. *Bull. Seismol. Soc. Am.* **102**, 352–360 (2012).
3. Denolle, M. A. & Shearer, P. M. New perspectives on self-similarity for shallow thrust earthquakes. *J. Geophys. Res. Solid Earth* **121**, 6533–6565 (2016).
4. Passelègue, FrançoisX. et al. Dynamic rupture processes inferred from laboratory microearthquakes: dynamic processes of stick-slip. *J. Geophys. Res. Solid Earth* **121**, 4343–4365 (2016).
5. Ide, S., Beroza, G. C., Shelly, D. R. & Uchide, T. A scaling law for slow earthquakes. *Nature* **447**, 76–79 (2007).
6. Peng, Z. & Gomberg, J. An integrated perspective of the continuum between earthquakes and slow-slip phenomena. *Nat. Geosci.* **3**, 599–607 (2010).
7. Frank, W. B. & Brodsky, E. E. Daily measurement of slow slip from low-frequency earthquakes is consistent with ordinary earthquake scaling. *Sci. Adv.* **5**, eaaw9386 (2019).
8. Michel, S., Gualandi, A. & Avouac, J.-P. Similar scaling laws for earthquakes and Cascadia slow-slip events. *Nature* **574**, 522–526 (2019).
9. Abercrombie, R. E. & Rice, J. R. Can observations of earthquake scaling constrain slip weakening? *Geophys. J. Int.* **162**, 406–424 (2005).
10. Weng, H. & Ampuero, J.-P. Integrated rupture mechanics for slow slip events and earthquakes. *Nat. Commun.* **13**, 7327 (2022).
11. Bletery, Q. et al. Characteristics of secondary slip fronts associated with slow earthquakes in Cascadia. *Earth Planet. Sci. Lett.* **463**, 212–220 (2017).
12. Ross, Z. E., Cochran, E. S., Trugman, D. T. & Smith, J. D. 3D fault architecture controls the dynamism of earthquake swarms. *Science* **368**, 1357–1361 (2020).
13. Holtkamp, S. G. & Brudzinski, M. R. Earthquake swarms in circum-Pacific subduction zones. *Earth Planet. Sci. Lett.* **305**, 215–225 (2011).
14. De Barros, L., Cappa, F., Deschamps, A. & Dublanchet, P. Imbricated aseismic slip and fluid diffusion drive a seismic swarm in the Corinth Gulf, Greece. *Geophys. Res. Lett.* **47**, (2020).
15. Godano, M. et al. The October–November 2010 earthquake swarm near Sampeyre (Piedmont region, Italy): A complex multicluster sequence. *Tectonophysics* **608**, 97–111 (2013).
16. Jenatton, L., Guiguet, R., Thouvenot, F. & Daix, N. The 16,000-event 2003–2004 earthquake swarm in Ubaye (French Alps). *J. Geophys. Res.* **112**, B11304 (2007).
17. Kraft, T., Wassermann, J. & Igel, H. High-precision relocation and focal mechanism of the 2002 rain-triggered earthquake swarms at Mt Hochstaufen, SE Germany. *Geophys. J. Int.* **167**, 1513–1528 (2006).
18. Fischer, T. et al. Intra-continental earthquake swarms in West-Bohemia and Vogtland: a review. *Tectonophysics* **611**, 1–27 (2014).
19. Albaric, J. et al. Monitoring of induced seismicity during the first geothermal reservoir stimulation at Paralana, Australia. *Geothermics* **52**, 120–131 (2014).
20. Block, L. V., Wood, C. K., Yeck, W. L. & King, V. M. The 24 January 2013 ML 4.4 Earthquake near Paradox, Colorado, and its relation to deep well injection. *Seismol. Res. Lett.* **85**, 609–624 (2014).
21. Charléty, J. et al. Large earthquakes during hydraulic stimulations at the geothermal site of Soultz-sous-Forêts. *Int. J. Rock. Mech. Min. Sci.* **44**, 1091–1105 (2007).
22. Ellsworth, W. L. Injection-induced earthquakes. *Science* **341**, 1225942 (2013).
23. Hatch, R. L., Abercrombie, R. E., Ruhl, C. J. & Smith, K. D. Evidence of aseismic and fluid-driven processes in a small complex seismic Swarm Near Virginia City, Nevada. *Geophys. Res. Lett.* **47**, (2020).
24. Cabrera, L., Poli, P. & Frank, W. B. Tracking the spatio-temporal evolution of foreshocks preceding the Mw 6.1 2009 L'Aquila Earthquake. *JGR Solid Earth* **127**, (2022).
25. Chen, X. & Shearer, P. M. California foreshock sequences suggest aseismic triggering process. *Geophys. Res. Lett.* **40**, 2602–2607 (2013).
26. Kato, A. & Nakagawa, S. Multiple slow-slip events during a foreshock sequence of the 2014 Iquique, Chile M_w 8.1 earthquake. *Geophys. Res. Lett.* **41**, 5420–5427 (2014).
27. Parotidis, M. Evidence for triggering of the Vogtland swarms 2000 by pore pressure diffusion. *J. Geophys. Res.* **110**, B05S10 (2005).
28. Goebel, T. H. W. & Brodsky, E. E. The spatial footprint of injection wells in a global compilation of induced earthquake sequences. *Science* **361**, 899–904 (2018).
29. Fischer, T. & Hainzl, S. The Growth of Earthquake Clusters. *Front. Earth Sci.* **9**, 638336 (2021).
30. Danré, P., De Barros, L., Cappa, F. & Ampuero, J. Prevalence of aseismic slip linking fluid injection to natural and anthropogenic seismic Swarms. *JGR Solid Earth* **127**, (2022).
31. Danré, P., Garagash, D., De Barros, L., Cappa, F. & Ampuero, J. Control of seismicity migration in earthquake swarms by injected fluid volume and aseismic crack propagation. *J. Geophys. Res.: Solid Earth* **129**, e2023JB027276 (2024).
32. Roland, E. & McGuire, J. J. Earthquake swarms on transform faults. *Geophys. J. Int.* **178**, 1677–1690 (2009).
33. Shapiro, S. A., Huenges, E. & Borm, G. Estimating the crust permeability from fluid-injection-induced seismic emission at the KTB site. *Geophys. J. Int.* **131**, F15–F18 (1997).
34. Fischer, T., Hainzl, S. & Vlček, J. Fast migration episodes within earthquake swarms. *Geophys. J. Int.* **235**, 312–325 (2023).
35. Passarelli, L., Selvadurai, P. A., Rivalta, E. & Jónsson, S. The source scaling and seismic productivity of slow slip transients. *Sci. Adv.* **7**, eabg9718 (2021).

36. De Barros, L., Wynants-Morel, N., Cappa, F. & Danré, P. Migration of fluid-induced seismicity reveals the seismogenic state of faults. *JGR Solid Earth* **126**, (2021).
37. Chen, X., Shearer, P. M. & Abercrombie, R. E. Spatial migration of earthquakes within seismic clusters in Southern California: Evidence for fluid diffusion: spatial migration of seismic clusters. *J. Geophys. Res.* **117**, n/a-n/a (2012).
38. Ruhl, C. J., Abercrombie, R. E., Smith, K. D. & Zaliapin, I. Complex spatiotemporal evolution of the 2008 M_w 4.9 Mogul earthquake swarm (Reno, Nevada): Interplay of fluid and faulting. *J. Geophys. Res. Solid Earth* **121**, 8196–8216 (2016).
39. Yoshida, K. et al. Updip fluid flow in the crust of the Northeastern Noto Peninsula, Japan, triggered the 2023 M_w 6.2 Suzu earthquake during swarm activity. *Geophys. Res. Lett.* **50**, e2023GL106023 (2023).
40. Ruiz, S. et al. Nucleation Phase and Dynamic Inversion of the M_w 6.9 Valparaíso 2017 Earthquake in Central Chile: M_w 6.9 Valparaíso 2017 Earthquake. *Geophys. Res. Lett.* **44**, 10,290–10.297 (2017).
41. Lohman, R. B. & McGuire, J. J. Earthquake swarms driven by aseismic creep in the Salton Trough, California: Obsidian Buttes Swarm. *J. Geophys. Res.* **112**, (2007).
42. Sirorattanakul, K. et al. The 2020 Westmorland, California Earthquake Swarm as Aftershocks of a Slow Slip Event Sustained by Fluid Flow. *JGR Solid Earth* **127**, (2022).
43. De Barros, L., Danré, P., Garagash, D., Cappa, F. & Lengliné, O. Systematic observation of a seismic back-front during fluid injection in both natural and anthropogenic earthquake swarms. *Earth Planet. Sci. Lett.* **641**, 118849 (2024).
44. Amezawa, Y., Maeda, T. & Kosuga, M. Migration diffusivity as a controlling factor in the duration of earthquake swarms. *Earth Planets Space* **73**, 1–11 (2021).
45. Socquet, A. et al. An 8 month slow slip event triggers progressive nucleation of the 2014 Chile megathrust: Progressive Nucleation Of Megathrust. *Geophys. Res. Lett.* **44**, 4046–4053 (2017).
46. Guglielmi, Y., Cappa, F., Avouac, J.-P., Henry, P. & Elsworth, D. Seismicity triggered by fluid injection-induced aseismic slip. *Science* **348**, 1224–1226 (2015).
47. Wynants-Morel, N., Cappa, F., De Barros, L. & Ampuero, J. Stress perturbation from aseismic slip drives the seismic front during fluid injection in a permeable fault. *J. Geophys. Res. Solid Earth* **125**, (2020).
48. Bhattacharya, P. & Viesca, R. C. Fluid-induced aseismic fault slip outpaces pore-fluid migration. *Science* **364**, 464–468 (2019).
49. Gualandi, A. et al. Aseismic deformation associated with an earthquake swarm in the northern Apennines (Italy): Aseismic Swarm Related Deformation. *Geophys. Res. Lett.* **44**, 7706–7714 (2017).
50. Hamiel, Y., Baer, G., Kalindekafe, L., Dombola, K. & Chindandali, P. Seismic and aseismic slip evolution and deformation associated with the 2009-2010 northern Malawi earthquake swarm, East African Rift: *The 2009-2010 northern Malawi earthquake swarm. Geophysical Journal International* https://doi.org/10.1111/j.1365-246X.2012.05673.x. (2012)
51. Passarelli, L. et al. Scaling and spatial complementarity of tectonic earthquake swarms. *Earth Planet. Sci. Lett.* **482**, 62–70 (2018).
52. Uchida, N. Detection of repeating earthquakes and their application in characterizing slow fault slip. *Prog. Earth Planet Sci.* **6**, 40 (2019).
53. Danré, P., De Barros, L. & Cappa, F. Inferring fluid volume during earthquake swarms using seismic catalogues. *Geophys. J. Int.* **232**, 829–841 (2023).
54. Ide, S. & Beroza, G. C. Slow earthquake scaling reconsidered as a boundary between distinct modes of rupture propagation. *Proc. Natl. Acad. Sci. USA* **120**, e2222102120 (2023).
55. Supino, M. et al. Self-similarity of low-frequency earthquakes. *Sci. Rep.* **10**, 6523 (2020).
56. Ojeda, J. et al. Seismic and aseismic slip during the 2006 Copiapó swarm in North-Central Chile. *J. South Am. Earth Sci.* **123**, 104198 (2023).
57. Wicks, C. et al. InSAR observations of aseismic slip associated with an earthquake swarm in the Columbia River flood basalts. *J. Geophys. Res.* **116**, B12304 (2011).
58. Cauchie, L., Lengliné, O. & Schmittbuhl, J. Seismic asperity size evolution during fluid injection: case study of the 1993 Soultz-sous-Forêts injection. *Geophys. J. Int.* **221**, 968–980 (2020).
59. Mukuhira, Y., Uno, M. & Yoshida, K. Slab-derived fluid storage in the crust elucidated by earthquake swarm. *Commun. Earth Environ.* **3**, 286 (2022).
60. Eyre, T. S. et al. The role of aseismic slip in hydraulic fracturing–induced seismicity. *Sci. Adv.* **5**, eaav7172 (2019).
61. Scholz, C. H. Earthquakes and friction laws. *Nature* **391**, 37–42 (1998).
62. Kuna, V. M., Nábělek, J. L. & Braunmiller, J. Mode of slip and crust–mantle interaction at oceanic transform faults. *Nat. Geosci.* **12**, 138–142 (2019).
63. Herrmann, M., Kraft, T., Tormann, T., Scarabello, L. & Wiemer, S. A consistent high-resolution catalog of induced seismicity in basel based on matched filter detection and tailored post-processing. *J. Geophys. Res. Solid Earth* **124**, 8449–8477 (2019).
64. Hillers, G. et al. Noise-based monitoring and imaging of aseismic transient deformation induced by the 2006 Basel reservoir stimulation. *Geophysics* **80**, KS51–KS68 (2015).
65. Bartlow, N. M., Miyazaki, S., Bradley, A. M. & Segall, P. Space-time correlation of slip and tremor during the 2009 Cascadia slow slip event: Cascadia Slow Slip And Tremor Migration. *Geophys. Res. Lett.* **38** (2011).
66. Houston, H., Delbridge, B. G., Wech, A. G. & Creager, K. C. Rapid tremor reversals in Cascadia generated by a weakened plate interface. *Nat. Geosci.* **4**, 404–409 (2011).

Acknowledgements

This work was supported by the ANR INSeis under contract ANR-22-CE49-0018 (L.D.B.).

Author contributions

Conceptualization: P.D., L.D.B., F.C., L.P. Methodology: P.D., L.D.B., F.C., L.P. Investigation: P.D. Visualization: P.D. Funding acquisition: L.D.B. Project administration: L.D.B., F.C. Supervision: L.D.B., F.C., L.P. Writing—original draft: P.D. Writing—review & editing: P.D., L.D.B., F.C., L.P.

Competing interests

The authors declare no competing interests.

Additional information

Supplementary information The online version contains supplementary material available at https://doi.org/10.1038/s41467-024-53285-3.

Correspondence and requests for materials should be addressed to Philippe Danré.

Peer review information *Nature Communications* thanks the anonymous reviewer(s) for their contribution to the peer review of this work. A peer review file is available.